ChemBioChem

Full Papers
doi.org/10.1002/cbic.202100437

Chemistry
Europe
European Chemical
Societies Publishing

www.chembiochem.org

VIP *Very Important Paper*

Visible-Light Removable Photocaging Groups Accepted by MjMAT Variant: Structural Basis and Compatibility with DNA and RNA Methyltransferases

Aileen Peters,[a] Eric Herrmann,[a] Nicolas V. Cornelissen,[a] Nils Klöcker,[a] Daniel Kümmel,*[a] and Andrea Rentmeister*[a]

Methylation and demethylation of DNA, RNA and proteins constitutes a major regulatory mechanism in epigenetic processes. Investigations would benefit from the ability to install photo-cleavable groups at methyltransferase target sites that block interactions with reader proteins until removed by non-damaging light in the visible spectrum. Engineered methionine adenosyltransferases (MATs) have been exploited in cascade reactions with methyltransferases (MTases) to modify biomolecules with non-natural groups, including first evidence for accepting photo-cleavable groups. We show that an engineered MAT from *Methanocaldococcus jannaschii* (PC-MjMAT) is 308-fold more efficient at converting *ortho*-nitrobenzyl-(ONB)-homo-cysteine than the wildtype enzyme. PC-MjMAT is active over a broad range of temperatures and compatible with MTases from mesophilic organisms. We solved the crystal structures of wildtype and PC-MjMAT in complex with AdoONB and a red-shifted derivative thereof. These structures reveal that aromatic stacking interactions within the ligands are key to accommodating the photocaging groups in PC-MjMAT. The enlargement of the binding pocket eliminates steric clashes to enable AdoMet analogue binding. Importantly, PC-MjMAT exhibits remarkable activity on methionine analogues with red-shifted ONB-derivatives enabling photo-deprotection of modified DNA by visible light.

Introduction

Methylation of biomolecules like DNA, RNA and proteins is a major regulatory mechanism involved in epigenetic and epitranscriptomic processes.[1] Numerous enzymes with the ability to introduce and reverse epigenetic marks have been identified. Histones are methylated on lysines and arginines, yielding different methylation states.[1c] In nucleic acids, DNA methyltransferases catalyze the installation of a methyl group at the N^4 or C5 position of cytosines and the N^6 position of adenines.[2] RNA methyltransferases act on many different positions in tRNAs and rRNAs.[3] In eukaryotic mRNAs, the N7 methylation of guanine is a hallmark of the 5′ cap and required for translation.[4] The most abundant internal modification in mRNAs is the methylation at the N^6 position of adenine.[1d,5]

The modifications lead to alterations of contacts between DNA and histones in chromatin and provide docking sites for so-called reader proteins, such as the methyl-CpG-binding domains (MBD) for DNA or the YTH domains for RNA.[6] The methyl group can in many cases be removed by demethylases, erasing the epigenetic or epitranscriptomic mark.[1b,6c] These enzymes are typically dioxygenases, like the TET enzymes (for DNA) or FTO and AlkBH5 (for RNA), oxidizing the methyl group to hydroxymethyl or higher oxidation states. The removal of m^5C from CpG islands in promoter regions of DNA is a key regulatory mechanism leading to increase of transcription.[1b] In mRNA, demethylation of m^6A has been observed, however, the actual role in epitranscriptomics is still debated.[6c,7]

S-Adenosyl-L-methionine (AdoMet) is the co-substrate of most methyltransferases (MTases) and thus the main methyl source.[8] Synthetic AdoMet analogues are also accepted by a number of promiscuous MTases or engineered variants.[9] AdoMet analogues and AdoMet-based inhibitors have been used as tools to study the mechanism and function of MTases.[10] It was shown that M.TaqI, a prokaryotic DNA MTase targeting the N^6 of adenine in the recognition sequence 5′-TCGA*-3′[11] accepts a number of AdoMet analogues that are extended at the nucleobase, the sulfonium center or both.[2,9a,b,12] In particular, the AdoMet analogues with extended carbon chains (e.g. alkyl, alkenyl and alkynyl groups) replacing the methyl group at the sulfonium center proved valuable for labeling and isolation of modified MTase target sites.[9a,d,g,13] Seminal work by the Luo group combined AdoMet analogues with histone MTases to identify their target proteins via click chemistry.[9j,14] In the field of DNA and RNA MTases, clickable AdoMet analogues proved suitable for labeling, isolation and preparation of libraries for next generation sequencing.[9b,c,e,f,h,15]

Furthermore, we and others recently demonstrated that AdoMet analogues in combination with suitable MTases are

[a]   A. Peters, E. Herrmann, N. V. Cornelissen, N. Klöcker, Prof. Dr. D. Kümmel,
      Prof. Dr. A. Rentmeister
      Department of Chemistry and Pharmacy
      Institute of Biochemistry, University of Münster
      Corrensstr. 36, 48149 Münster (Germany)
      E-mail: daniel.kuemmel@uni-muenster.de
              a.rentmeister@uni-muenster.de

broadly applicable for transfer of photo-cleavable (PC) groups to DNA, RNA and the mRNA 5′ cap.[12a,b,15d,16] This post-synthetic enzymatic modification and the light-induced removal provide methodology for site-specific "writing" and "erasing" marks on long DNA or RNA at natural MTase sites.

However, the chemical synthesis of AdoMet analogues is rather inefficient and yields both epimers at the sulfonium center.[9a,g] Furthermore, AdoMet is unstable in aqueous solution[8] and degrades to methylthioadenosine (MTA) via intramolecular cyclization[17] (Figure 1A, Figure S1). Moreover, AdoMet analogues are not cell permeable, limiting cellular applications.[17] In the biosynthetic pathway, methionine adenosyltransferases (MATs) convert methionine (**1a**) and ATP to AdoMet[13c] (Figure 1A). This strategy can be harnessed for the chemo-enzymatic generation of AdoMet analogues from synthetic methionine and/or ATP analogues[17,18] (Figure 1B) to address the above-mentioned limitations. Human cells can be metabolically labeled with propargyl-selenohomocysteine to generate the propargyl-containing AdoMet analogue and identify RNA methylation sites on adenosines.[15b] Human MAT2

has been engineered to accept the bulkier (E)-hex-2-en-5-ynyl homocysteine and identify histone methylation marks.[19]

To make AdoMet analogues with PC groups enzymatically accessible and as a first step towards intracellular application, we engineered MAT from *Cryptosporidium hominis* and showed that the RNA 5′ cap can be equipped with PC-groups in cascade reactions. As the enzyme showed low activity in cascades with thermophilic enzymes, we introduced the homologous mutations into the MAT from *Methanocaldococcus jannaschii*. With this L147A/I351A variant (termed PC-MjMAT), we achieved site-specific reversible modification of DNA with the ONB group in a cascade reaction with M.TaqI.[20]

While this was an important proof-of-concept, several limitations remained. Red-shifted photo-caging groups would be required for application in cells to study processes without triggering photo-toxicity or stress reactions. Compatibility with ambient temperatures and high MAT activity in cascades with enzymes from mesophilic eukaryotes like mammals would be necessary.

We therefore sought to further investigate MjMAT variant L147A/I351A for the ability to efficiently generate AdoMet
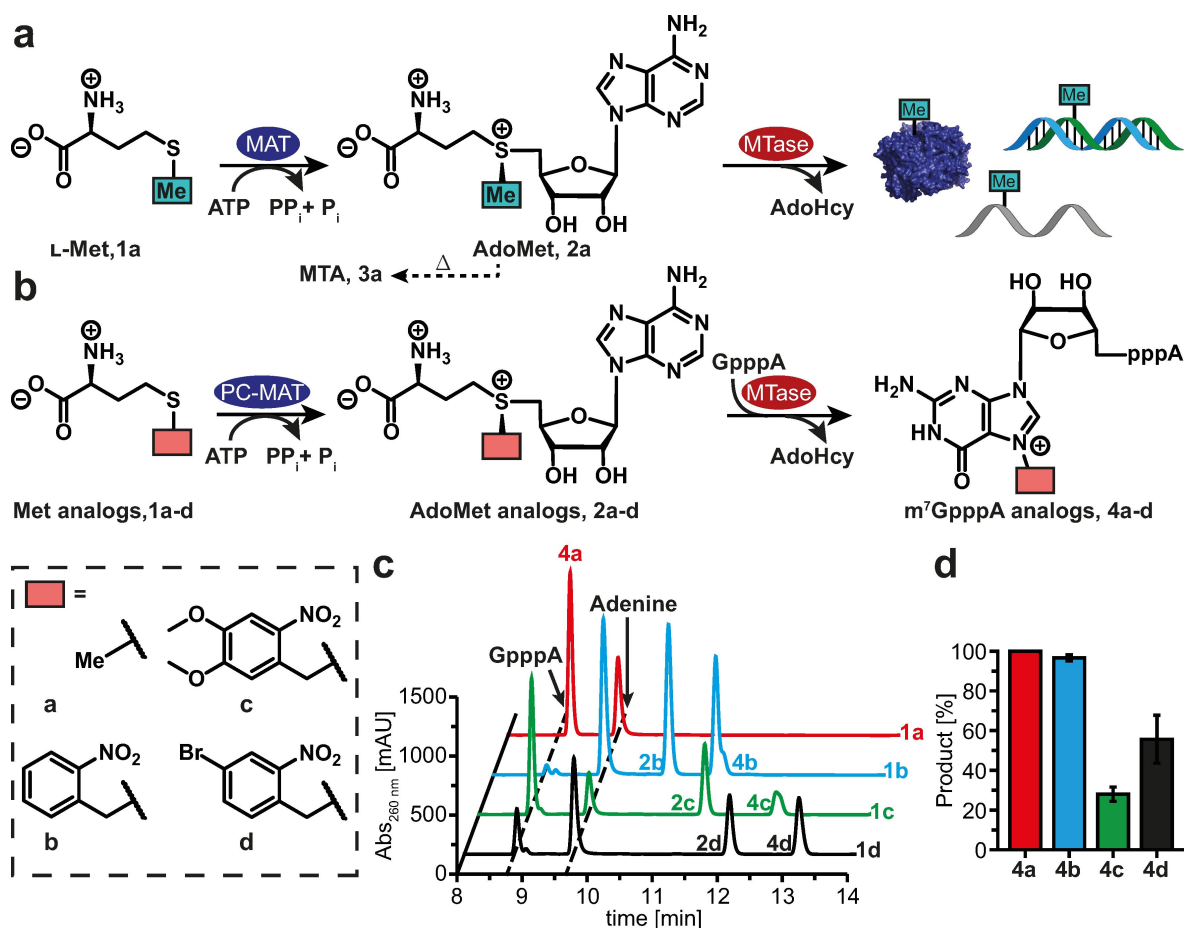

Figure 1. Enzymatic cascade reaction of methionine adenosyltransferase (MAT) and methyltransferase (MTase). a) Enzymatic methylation of biomolecules (DNA, RNA, proteins) via cascade reaction of methionine adenosyltransferase (MAT) and methyltransferase (MTase) starting from L-methionine (**1a**). Degradation of S-adenosyl-L-methionine (AdoMet, **2a**) to methylthioadenosine (MTA, **3a**) can be induced by heat. b) Enzymatic modification of the N7 position of the mRNA 5′-cap analogue GpppA by PC-MjMAT/Ecm1 cascade starting from **1a–d**. c) HPLC analysis of reactions with indicated substrates (**1a–d**) after incubation at 37 °C for 90 min. d) Evaluation of (c) showing formation of the modified cap analogue (**4a–d**) after 90 min.

ChemBioChem

Full Papers
doi.org/10.1002/cbic.202100437

Chemistry
Europe
European Chemical
Societies Publishing

analogues with red-shifted photocaging groups and its activity at ambient temperature, which would be important for application in mammalian systems in future epigenetic studies. We also aimed to get structural insights into MjMAT and the PC-MjMAT. No crystal structure is available to date and we had previously relied on a structural homology model, despite the relatively low sequence identity of 51% and the knowledge that archaeal MAT can significantly diverge from bacterial and eukaryotic ones.[21] Structural knowledge of MAT variants would help to understand the molecular basis of AdoONB accommodation and to guide further decisions for engineering.

Results and Discussion

PC-MjMAT is highly active at 37 °C and compatible with mesophilic MTase in cascade reactions

We had previously shown that PC-MjMAT can use **1 b** in a cascade reaction with M.TaqI at high temperature (65 °C).[20] However, for application in epigenetic studies of human cells, activity at 37 °C is required. To assess whether PC-MjMAT that originates from a thermophilic organism would also be compatible with enzymes from mesophilic organisms, we tested its activity at 37 °C in a cascade reaction with Ecm1, a highly promiscuous mRNA cap guanine N7 MTase from the mesophilic organism *Encephalitozoon cuniculi*.[9h,16, 18e, 20, 22] Starting from L-methionine (**1 a**) or analogues (**1 b–d**), the AdoMet (**2 a**) or analogues (**2 b–d**) were formed *in situ* and the 5′ cap analogue GpppA was modified (Figure 1A/B, Figure S2).

HPLC analysis showed that the natural substrate **1 a** resulted in complete conversion of GpppA to **4 a** after 90 min (Figure 1C/D, Figures S3/S4). Using 2-nitrobenzyl-D,L-homocysteine (ONB-Hcy, **1 b**) yielded remarkable 97% of **4 b** under otherwise identical conditions (Figure 1C/D, Figures S3/S4). The sterically more demanding red-shifted ONB-derivatives 4,5-dimethoxy-2-nitrobenzyl-homocysteine (DMNB-Hcy, **1 c**) and 4-bromo-2-nitrobenzyl-homocysteine (pBrONB-Hcy, **1 d**) were also efficiently converted, yielding 28% of **4 c** and 56% of **4 d**, respectively (Figure 1C/D, Figures S3/S4). Taken together, these data show that methionine analogues with PC-groups can be converted by PC-MjMAT at ambient temperature, despite the enzyme originating from a thermophilic organism. This observation is important for future application in human cells.

AdoMet is a product inhibitor of MAT enzymes with K_i values in the range of 10 μM.[18b] A key reason for the use of MAT/MTase cascade reactions is to circumvent this product inhibition. Interestingly, when we used PC-MjMAT, we detected significant amounts of AdoMet (**2 a**) (Figure S3) or its analogues (**2 b–d**) in MAT/Ecm1 cascade reactions (Figure 1C), suggesting that product inhibition might be less prominent in this case. We had not observed detectable amounts of **2 a–d** in HPLC runs in our previous studies using different MATs, such as hMAT (human MAT)[18d] or ChMAT (MAT from *Cryptosporidium hominis*)[20] variants under similar conditions.

For wildtype MjMAT a K_i value for AdoMet at ~2 mM was reported, indicating that the product inhibition is ~200 times

weaker than for other MAT enzymes.[18b] Our data suggest that for PC-MjMAT, the same holds true for AdoMet analogues, resulting in the accumulation of high amounts of **2 b–d** (Figure 1C, Figure S3).

PC-MjMAT/MTase cascade can modify DNA with visible-light removable photocaging groups

A particularly interesting application of MAT/MTase cascades is sequence-specific installation and light-induced removal of photocaging groups in DNA. Recently, we reported that PC-MjMAT can be used in cascade reactions with M.TaqI - a DNA MTase targeting N6A in the recognition sequence 5′-TCGA-3′[11] - to modify specific sequences in plasmid DNA using **1 b**.[20] The resulting ONB-modification could be completely removed by irradiation with light of 365 nm for 90 s (Figure S5A), rendering the plasmid susceptible to enzymatic degradation with the restriction enzyme R.TaqI.[20] This was an important finding, however, irradiation of biological systems with light of 365 nm causes cell stress and can lead to unwanted photo-chemistry, which reduces cell viability depending on the intensity and duration of irradiation. Hence, it is generally agreed that photo-cleavable groups that can be removed by red-shifted or visible light (>400 nm) are preferable for applications in biological systems.[23]

We therefore sought to transfer red-shifted ONB-derivatives to plasmid DNA in cascade reactions to protect it from enzymatic degradation (Figure 2A) and achieve photo-deprotection at wavelengths >400 nm. To this end, we tested methionine analogues **1 c–d** at 37 °C in PC-MjMAT/M.TaqI cascades with the pUC19 plasmid, containing four M.TaqI target sites on each strand (Figure 2). For both substrates, gel analysis of the treated pUC19 plasmid showed that the DNA was successfully protected from degradation by R.TaqI, indicating efficient transfer and complete modification of the plasmid (lane 4 in Figure 2B/C). Two positive controls, containing either the linearized plasmid (lane 1) or plasmid methylated using L-methionine in the cascade reaction (lane 3) show a band at the same length (Figure 2B/C).

Next, we irradiated the completely protected pUC19 plasmids for 90 s with light of 365 nm, 405 nm, or 420 nm, respectively. To analyze whether photo-deprotection had occurred, the plasmids were then treated with R.TaqI and NdeI. Subsequent gel analysis revealed that the plasmid DNA was degraded (lanes 5–7, Figure 2B/C), similar to unmethylated plasmid (lane 2), indicating that the photo-cleavable groups had been removed (Figure 2B/C). The ability to enzymatically generate and transfer photo-cleavable groups to DNA that can be removed at ≥405 nm is an important step for cellular applications and epigenetic studies.

As we noticed that the cascade reaction with PC-MjMAT/M.TaqI is remarkably efficient, we were curious to challenge the system and modify phage ʎ-DNA, which is 48,502 bp long and contains 121 M.TaqI target sites on each strand. Indeed, ʎ-DNA treated with PC-MjMAT/M.TaqI and **1 b** was protected from restriction by R.TaqI, similar to results obtained with L-

ChemBioChem

Full Papers
doi.org/10.1002/cbic.202100437

**Chemistry
Europe**
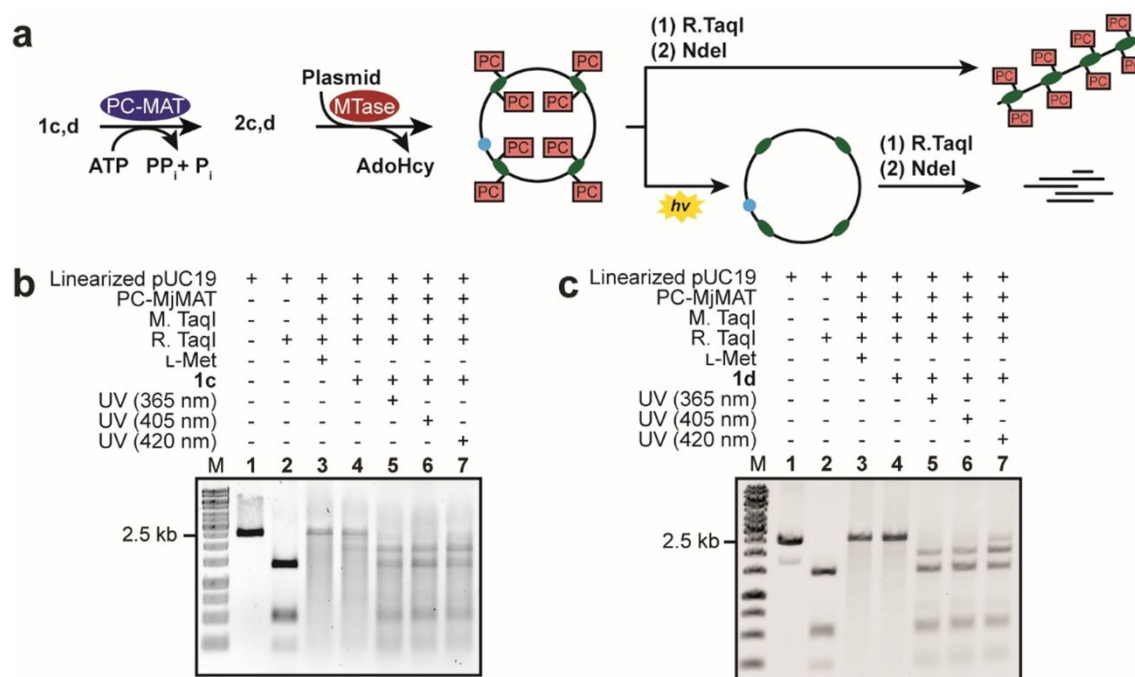European Chemical
Societies Publishing

Figure 2. Reversible photocaging of plasmid DNA via PC-MjMAT/M.TaqI cascade reaction. a) Modification restriction assay: Reversible modification of DNA by targeting MTase sites in the cascade reaction of PC-MjMAT and M.TaqI ("writing"). After cleavage of the PC-group ("erasing"), the unmodified plasmid can be degraded by R.TaqI. b, c) Analysis of the cascade reaction starting from **1c** (b) and **1d** (c). Irradiation for 90 s at indicated wavelengths.

methionine (Figure S5B). After irradiation with light, the **1b**-treated λ-DNA became accessible to enzymatic fragmentation by R.TaqI (similar to untreated λ-DNA), indicating removal of the PC-groups.

Taken together, these data show that PC-MjMAT is remarkably efficient in generation of AdoMet analogues **2c–d** bearing photocaging groups, which are red-shifted derivatives of the widely used ONB-group. The PC-groups transferred from **1c–d** can be removed by irradiation with light of 405 nm and even 420 nm. This red-shift compared to the 365 nm required for ONB-removal provides an important improvement towards compatibility with cellular systems.

Temperature profile and kinetic studies of PC-MjMAT

To get a more comprehensive overview of the temperature-activity relationship of PC-MjMAT, we measured the PC-MjMAT activity at nine different temperatures ranging from 20 °C to 100 °C. We used a previously described HPLC-based assay[17,20] detecting the degradation product methylthioadenosine (MTA, **3a**) or the respective analogue 2-nitrobenzylthioadenosine (ONB-TA, **3b**) (Figure 1A, Figure S6). We shortened the reaction time to 15 min to avoid potential perturbations by product inhibition of AdoMet (Figure S6).

Analysis of the activity at different temperatures showed that PC-MjMAT is active over a broad range of temperatures with an optimal temperature at 80 °C (Figure 3A, Figure S7). The

observation that PC-MjMAT retains high activity at ambient temperature - e.g. 30% relative activity at 37 °C (Figure 3A) - is important for two reasons. First, it allows application of PC-MjMAT in a wide range of cascade reactions, not limited to MTases from thermophilic organisms, but also with MTases from mesophilic organisms. Second, we observed that AdoMet is more stable at lower temperatures, resulting in more efficient photocaging at 37 °C compared to 65 °C. This is best illustrated by comparing the DNA photoprotection using the PC-MjMAT/MTaqI cascade and **1c**, which leads to complete protection at 37 °C (Figure 2B) but not at 65 °C (Figure S5C), although both enzymes are thermostable. We attribute this to the competing degradation of AdoMet analogues reducing the substrate concentration available to the MTase.

To assess the improvements in catalytic efficiency of PC-MjMAT for **1b**, we determined the kinetic parameters from initial velocity measurements. To this end, we used the HPLC-based assay described above for 10 different concentrations of **1b** (0–30 mM) and measured formation of **3b** after 3 min at 80 °C (Figure 3B, Figures S8/S9). From non-linear regression (Michaelis-Menten fit) a maximal velocity (v_{max}) of 140 µM/min, a Michaelis-Menten constant (K_M) of 1.59 mM and a turnover number (k_{cat}) of 14 min^{-1} (Figure 3B) were calculated.

To quantify the improvement of PC-MjMAT compared to the wildtype regarding the ability to convert **1b**, we performed the ONB-TA assay at high temperature (1 h, 65 °C) to ensure rapid formation of **3b** and avoid production inhibition. While the wildtype enzyme yielded barely detectable amounts of **3b**,
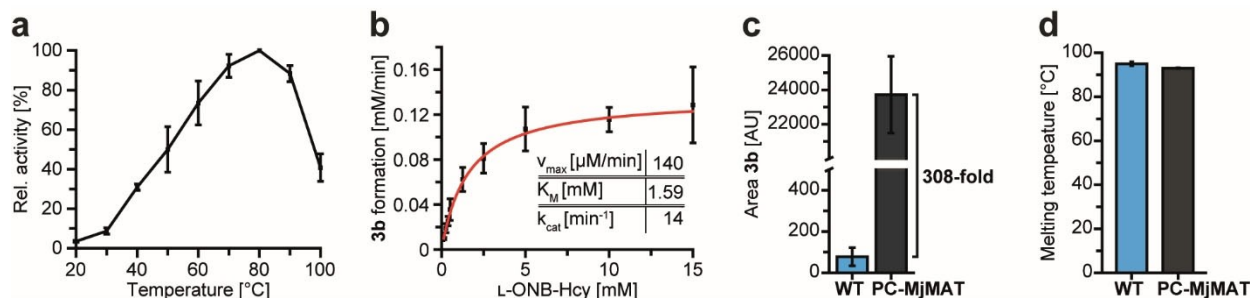
ChemBioChem

Full Papers
doi.org/10.1002/cbic.202100437

**Chemistry
Europe**
European Chemical
Societies Publishing

Figure 3. Characterization of PC-MjMAT. a) Temperature-activity profile of PC-MjMAT. Data are normalized to the maximum activity (T = 80 °C). b) Kinetic assay of PC-MjMAT by varying ONB-Hcy **1 b** concentration at 80 °C and after 3 min reaction time. Kinetic parameters were determined by non-linear fitting via Origin. c) Comparison of WT and PC-MjMAT regarding to the activity on ONB-Hcy **1 b**. A 308-fold improvement in conversion was determined after 1 h reaction time. d) Comparison of the thermostability of PC-MjMAT and WT-MjMAT as exemplified for condition G1 (RUBIC buffer screen, Figure S11, Table S1). Data and error bars show average and standard deviation of three independent experiments.

PC-MjMAT showed high conversion, which corresponds to a ~308-fold improvement (Figure 3C, Figure S10).

Structural characterization of wildtype MjMAT and PC-MjMAT

To find out whether the two substitutions in PC-MjMAT had compromised the thermostability of the enzyme, we performed thermal shift assays of both wildtype and PC-MjMAT in standard buffer (Figure 3D) and also tested different buffer conditions and pH values (Figure S11, Table S1). PC-MjMAT exhibited a slightly lower melting temperatures, but in the same range as WT-MjMAT, with $T_m > 90$ °C in most of the conditions tested. These data indicate that the substitutions L147A/I351A did not severely affect the thermostability of the enzyme and did not result in profoundly increased sensitivity to changes in pH or ionic strength.

Based on our findings and reports in the literature,[18b] PC-MjMAT is a remarkable enzyme that shows a broad substrate tolerance and low product inhibition compared to homologous MAT enzymes. To better understand the mechanistic basis and provide a structural framework for further improvement of this enzyme, we attempted its crystallization with PC substrates. Crystallization of WT-MjMAT has been reported,[18b] but no structure was described or deposited at the PDB.

We first crystallized wildtype (PDB ID: 7P83) and PC-MjMAT (PDB ID: 7P82) and obtained the apo-structures at 2.22 Å and 2.04 Å resolution, respectively (Figure S13, Table S2). Both structures are highly similar (rmsd 0.318 Å, Figure S13A), demonstrating that the double mutation L147A/I351A did not affect folding of MjMAT, and we will focus our discussion on PC-MjMAT. The asymmetric unit contains a PC-MjMAT homo-dimer and its architecture matches that of other crystallized MAT structures[24] with two active sites formed by the interface of the two monomers (Figure S13A). Access to the active site of MATs is regulated by a gating loop, which can adopt an open, usually partially unfolded conformation or a closed configuration that covers the entry path to the active site. The gating loops are fully folded in our MjMAT (WT and PC) structures.

Interestingly, the gating loop adopts the open conformation in one monomer and the closed conformation in the other (Figure S13C–E). To the best of our knowledge, a completely closed gating loop conformation at an empty active site has previously not been observed in other MATs.

To investigate how different PC-AdoMet analogues are bound by PC-MjMAT, we soaked PPP$_i$ and **2 b** into apo PC-MjMAT crystals and determined the ligand-bound structure at 2.05 Å resolution, respectively (PDB: 7P84) (Figure 4A, S14A/C). Binding of ligand did not change the structure of PC-MjMAT (rmsd 0.2 Å), and the gating loops still adopt the closed or open conformation, respectively, at the two active sites. The active site with the open gating loop only has PPP$_i$ bound, while the active site with the closed gating loop contains **2 b** and PPP$_i$. Ligand-bound crystals were not obtained by co-crystallization, but by soaking of apo crystals. Thus, the gating loop must have opened during the crystal soaking to allow diffusion of **2 b** and PPP$_i$ into their binding pocket and closed again to adopt the observed structure. This observation demonstrates that the closed conformation of the gating loop in the apo structure is not caused by crystal packing.

The closest homolog to MjMAT with known structure is the MAT from *Pyrococcus furiosus* (PfMAT), which is 63 % identical (Figure S12).[24c,25] However, the apo structures of PC-MjMAT and PfMAT deviate with an rmsd of 1.847 Å (Figure S13B), and the structures of PC-MjMAT with **2 b** and PfMAT with AdoMet[24c] also have an rmsd of 1.358 Å (Figure S15A). This is caused by different conformations of peripheral loops and, importantly, of the gating loops, which are all in the open conformation in PfMAT. There is substantial sequence divergence in the gating loops of MjMAT and PfMAT (Figure 4B), suggesting that functional differences between both enzymes could be linked to the mechanism of the gating loop. The principle architecture of the active site, in contrast, is conserved (Figure 4C). The adenine base is bound by a tyrosine (MjMAT Y273/PfMAT Y268) and an aspartate (MjMAT D146/PfMAT D141), and the methionine carboxyl group is coordinated by a conserved histidine (MjMAT H58/PfMAT H59). The only difference is the enlargement of the hydrophobic binding pocket resulting from the mutations
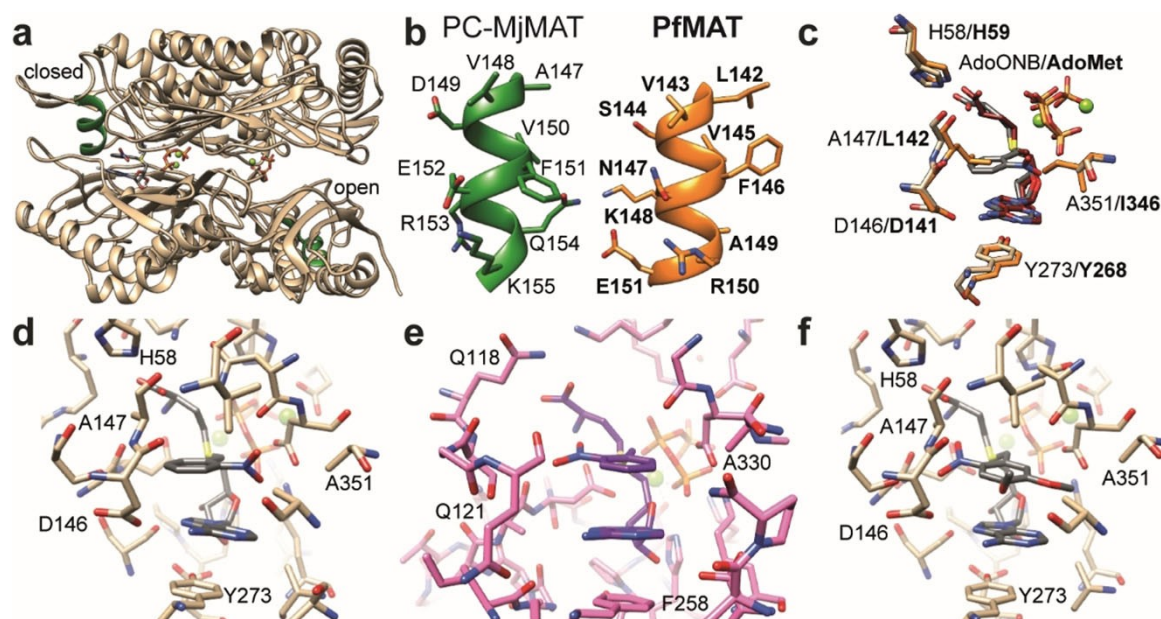
ChemBioChem

Full Papers
doi.org/10.1002/cbic.202100437

Chemistry Europe
European Chemical
Societies Publishing

Figure 4. Structural analysis of PC-MjMAT. a) Structure of the PC-MjMAT dimer (tan) in complex with **2b** (gray stick model). The gating loops are colored green. One active site is empty, with an open gating loop conformation, and a second binding site with a closed gating loop is occupied by **2b**. b) The PC-MjMAT gating loop (green, left) and PfMAT gating loop (orange, right) have divergent sequences. c) Superposition of the active sites of PC-MjMAT (tan) with **2b** (gray) and PfMAT (orange) with AdoMet (red). d) Binding of **2b** (gray) to the active site of PC-MjMAT (tan). e) Binding of **2b** (purple) to the active site of PC-ChMAT (pink). f) Binding of **2c** (gray) to the active site of PC-MjMAT (tan).

L147A/I351A in MjMAT that allow the accommodation of the sterically demanding ONB group (Figure 4C). We made the identical observations when we compared MjMAT to the MAT from *Sulfolobus solfataricus* (SsMAT),[24b] which is 51% identical (Figure S12).

The main interaction of the ONB group is via π stacking with the adenine base (Figure 4D). The nitro group faces the hydrophobic back of the binding pocket and does not make specific hydrogen bonding interactions. The binding of **2b** to PC-MjMAT is different than to PC-ChMAT, which we have investigated before,[20] where the nitro group is oriented towards the base of the gating loop (Figure 4E). This was surprising because the design of PC-ChMAT and PC-MjMAT was based on the same rationale. This finding indicates that there is a relatively large degree of promiscuity in the binding of aromatic ligands to PC-MATs.

Overall, the binding pocket of PC-MjMAT is slightly larger than of PC-ChMAT (Figure S15B), which explains why PC-MjMAT is also able to turn over larger substrates. We therefore also determined the structure of the 4,5-dimethoxy derivative **2c** at 1.71 Å resolution (PDB ID: 7P8 M) (Figures S15C, S14B/D). The DMNB moiety is also bound via π stacking with the adenine base (Figure 4 F). The nitro group is flipped compared to the PC-MjMAT complex with **2b** and is oriented towards the gating loop, similar to **2b** in complex with PC-ChMAT. This again suggests that the aromatic stacking is the relevant interaction to accommodate PC substrates in the MATs.

Conclusion

Characterization of the highly expressing MjMAT variant L147A/ I351A (PC-MjMAT) revealed that this variant efficiently converts methionine analogues with photo-cleavable groups and functions over a broad range of temperatures (T = 20–100 °C) and buffer conditions. PC-MjMAT retains the remarkable thermostability of the wildtype MjMAT (T$_m$ > 90 °C). In comparison to our previous work[20] where PC-ChMAT/Ecm1 cascade reaction yielded about 70% **4b** after 8 h of incubation, PC-MjMAT/Ecm1 can almost quantitatively modify the mRNA cap analogue GpppA within only 90 min (97% **4b**). Importantly, we could show that PC-MjMAT accepts methionine analogues with ONB-derivatives, which are red-shifted but sterically more demanding. Accordingly, the yields for PC-MjMAT/Ecm1 were doubled for **4c** (28% vs. ~15%) as well as **4d** (56% vs. ~24%), compared to previous work with PC-ChMAT/Ecm1.[20]

This activity on methionine analogues with red-shifted PC-groups (**1c–d**) allowed the efficient sequence-specific photo-caging of DNA by PC-MjMAT/M.TaqI cascade reactions and subsequent removal of the PC-groups with visible light (ƛ = 405–420 nm), an important step towards potential cellular applications.

Another attractive feature of PC-MjMAT is a low product inhibition by AdoMet analogues. For the first time, we observed accumulation of **2b–d** in cascade reactions. From previous work, it is known that MjMAT shows significantly less product inhibition by AdoMet compared to other MAT enzymes[18b] and that homologous substitutions to I351A in other MATs (e.g.

I317 in BsMAT, I303 in EcMAT) can reduce product inhibition.[18c,26] Minor product inhibition makes PC-MjMAT an interesting alternative for production of enantiomeric pure AdoMet and AdoMet analogues with photocaging groups by biotransformation. For such an application, the activity of PC-MjMAT at low temperature is particularly beneficial, as the low temperature reduces degradation of AdoMet and its analogues.

Finally, the crystal structures of the wildtype and the engineered methionine adenosyltransferase from *Methanocaldococcus jannaschii* provides insight into the mechanistic basis of these properties. To the best of our knowledge, this is the first report on structures of MjMAT. We observed that the gating loop of MjMAT can adopt the closed conformation even in the absence of substrate, which to our knowledge has not been observed in other MATs. This is also the only major difference between MjMAT and its closest homologs with known substrate-bound structure, PfMAT and SsMAT. Because MjMAT shows much lower product inhibition compared to SsMAT,[18b,27] we speculate that the closed gating loop in the apo form of MjMAT might be the mechanistic reason for its reduced product inhibition.

The structures of PC-MjMAT in complex with the AdoMet analogues **2b**–**c** show that aromatic stacking interactions within the ligands are key for the accommodation of photocaging groups in the active site. The ligands are coordinated via identical interactions like the natural substrate AdoMet through hydrogen bonds with the adenine base, the ribose and the amino and carboxyl groups. We observe no specific interactions with the nitro or methoxy groups of **2b** and **2c**. The enlargement of the binding pocket that eliminates steric clashes appears to be the sole requirement for AdoMet analogue binding. Thus, PC-MjMAT may also be useful for the generation of other AdoMet analogues with aromatic functionalities, like photo-crosslinkers[9g] or fluorophores.[28] The extraordinary thermostability of MjMAT is not compromised by the mutations in PC-MjMAT, which is encouraging to attempt further enlargement of the hydrophobic binding pocket. Based on our crystal structures, the substrate spectrum of MjMAT could thus be further extended. Our biochemical and structural work on the engineered PC-MjMAT characterizes this protein as an enzyme with high stability in a wide range of conditions, low product inhibition and extended substrate promiscuity. We expect that this protein will be very useful for a wide range of applications.

Acknowledgements

Conflict of Interest

The authors declare no conflict of interest.

Keywords: archaeal MAT · crystal structures · MjMAT · photocaging · SAM synthetase

[1] a) Y. Fu, D. Dominissini, G. Rechavi, C. He, *Nat. Rev. Genet.* **2014**, *15*, 293–306; b) M. V. Greenberg, D. Bourc'his, *Nat. Rev. Mol. Cell Biol.* **2019**, *20*, 590–607; c) R. J. Klose, Y. Zhang, *Nat. Rev. Mol. Cell Biol.* **2007**, *8*, 307–318; d) P. J. Hsu, H. Shi, C. He, *Genome Biol.* **2017**, *18*, 1–9.

[2] W. Fischle, D. Schwarzer, *ACS Chem. Biol.* **2016**, *11*, 689–705.

[3] Y. Motorin, M. Helm, *Wiley Interdiscip. Rev.: RNA* **2011**, *2*, 611–631.

[4] a) N. Sonenberg, A. G. Hinnebusch, *Cell* **2009**, *136*, 731–745; b) J. Marcotrigiano, A.-C. Gingras, N. Sonenberg, S. K. Burley, *Cell* **1997**, *89*, 951–961.

[5] K. W. Seo, R. E. Kleiner, *ACS Chem. Biol.* **2020**, *15*, 132–139.

[6] a) D. Schübeler, *Nature* **2015**, *517*, 321–326; b) S. Liao, H. Sun, C. Xu, *Genomics Proteomics Bioinf.* **2018**, *16*, 99–107; c) N. Liu, T. Pan, *Nat. Struct. Mol. Biol.* **2016**, *23*, 98–102.

[7] R. B. Darnell, S. Ke, J. E. Darnell, *RNA* **2018**, *24*, 262–267.

[8] J. Deen, C. Vranken, V. Leen, R. K. Neely, K. P. F. Janssen, J. Hofkens, *Angew. Chem. Int. Ed.* **2017**, *56*, 5182–5200; *Angew. Chem.* **2017**, *129*, 5266–5285.

[9] a) C. Dalhoff, G. Lukinavicius, S. Klimasauskas, E. Weinhold, *Nat. Chem. Biol.* **2006**, *2*, 31–32; b) G. Lukinavicius, V. Lapiene, Z. Stasevskij, C. Dalhoff, E. Weinhold, S. Klimasauskas, *J. Am. Chem. Soc.* **2007**, *129*, 2758–2759; c) Y. Motorin, J. Burhenne, R. Teimer, K. Koynov, S. Willnow, E. Weinhold, M. Helm, *Nucleic Acids Res.* **2011**, *39*, 1943–1952; d) J. M. Holstein, D. Stummer, A. Rentmeister, *Protein Eng. Des. Sel.* **2015**, *28*, 179–186; e) J. M. Holstein, D. Stummer, A. Rentmeister, *Chem. Sci.* **2015**, *6*, 1362–1369; f) J. M. Holstein, D. Schulz, A. Rentmeister, *Chem. Commun.* **2014**, *50*, 4478–4481; g) F. Muttach, F. Masing, A. Studer, A. Rentmeister, *Chem. Eur. J.* **2017**, *23*, 5988–5993; h) F. Muttach, N. Muthmann, D. Reichert, L. Anhauser, A. Rentmeister, *Chem. Sci.* **2017**, *8*, 7947–7953; i) K. Islam, W. Zheng, H. Yu, H. Deng, M. Luo, *ACS Chem. Biol.* **2011**, *6*, 679–684; j) K. Islam, I. Bothwell, Y. Chen, C. Sengelaub, R. Wang, H. Deng, M. Luo, *J. Am. Chem. Soc.* **2012**, *134*, 5909–5915.

[10] J. Zhang, Y. G. Zheng, *ACS Chem. Biol.* **2016**, *11*, 583–597.

[11] K. Goedecke, M. Pignot, R. S. Goody, A. J. Scheidig, E. Weinhold, *Nat. Struct. Biol.* **2001**, *8*, 121–125.

[12] a) L. Anhauser, F. Muttach, A. Rentmeister, *Chem. Commun.* **2018**, *54*, 449–451; b) M. Heimes, L. Kolmar, C. Brieke, *Chem. Commun.* **2018**, *54*, 12718–12721; c) C. Dalhoff, G. Lukinavičius, S. Klimašauskas, E. Weinhold, *Nat. Protoc.* **2006**, *1*, 1879–1886.

[13] a) I. R. Bothwell, M. Luo, *Org. Lett.* **2014**, *16*, 3056–3059; b) V. Masevičius, M. Nainytė, S. Klimašauskas, *Curr. Protoc. Nucleic Acid Chem.* **2016**, *64*, 1.36. 31–31.36. 13; c) T. D. Huber, B. R. Johnson, J. Zhang, J. S. Thorson, *Curr. Opin. Biotechnol.* **2016**, *42*, 189–197.

[14] a) I. R. Bothwell, K. Islam, Y. Chen, W. Zheng, G. Blum, H. Deng, M. Luo, *J. Am. Chem. Soc.* **2012**, *134*, 14905–14912; b) K. Islam, Y. Chen, H. Wu, I. R. Bothwell, G. J. Blum, H. Zeng, A. Dong, W. Zheng, J. Min, H. Deng, *Proc. Natl. Acad. Sci. USA* **2013**, *110*, 16778–16783; c) R. Wang, W. Zheng, H. Yu, H. Deng, M. Luo, *J. Am. Chem. Soc.* **2011**, *133*, 7648–7651.

[15] a) M. Mickutė, K. Kvederavičiūtė, A. Osipenko, R. Mineikaitė, S. Klimašauskas, G. Vilkaitis, *BMC Biol.* **2021**, *19*, 129; b) K. Hartstock, B. S. Nilges, A. Ovcharenko, N. V. Cornelissen, N. Pullen, A. M. Lawrence-Dorner, S. A. Leidel, A. Rentmeister, *Angew. Chem. Int. Ed.* **2018**, *57*, 6342–6346; *Angew. Chem.* **2018**, *130*, 6451–6455; c) G. V. Lukinavičius, M. Tomkuvienė, V. Masevičius, S. Klimašauskas, *ACS Chem. Biol.* **2013**, *8*, 1134–1139; d) A. Ovcharenko, F. P. Weissenboeck, A. Rentmeister, *Angew. Chem. Int. Ed.* **2021**, *60*, 4098–4103; *Angew. Chem.* **2021**, *133*, 4144–4149.

[16] L. Anhauser, N. Klocker, F. Muttach, F. Masing, P. Spacek, A. Studer, A. Rentmeister, *Angew. Chem. Int. Ed.* **2020**, *59*, 3161–3165; *Angew. Chem.* **2020**, *132*, 3186–3191.

[17] R. Wang, W. Zheng, M. Luo, *Anal. Biochem.* **2014**, *450*, 11–19.

[18] a) S. Singh, J. Zhang, T. D. Huber, M. Sunkara, K. Hurley, R. D. Goff, G. Wang, W. Zhang, C. Liu, J. Rohr, S. G. Van Lanen, A. J. Morris, J. S. Thorson, *Angew. Chem. Int. Ed.* **2014**, *53*, 3965–3969; *Angew. Chem.* **2014**, *126*, 4046–4050; b) Z. J. Lu, G. D. Markham, *J. Biol. Chem.* **2002**, *277*, 16624–16631; c) M. Dippe, W. Brandt, H. Rost, A. Porzel, J. Schmidt, L. A. Wessjohann, *Chem. Commun.* **2015**, *51*, 3637–3640; d) F. Muttach, A. Rentmeister, *Angew. Chem. Int. Ed.* **2016**, *55*, 1917–1920; *Angew. Chem.* **2016**, *128*, 1951–1954; e) N. V. Cornelissen, F. Michailidou, F. Muttach, K. Rau, A. Rentmeister, *Chem. Commun.* **2020**, *56*, 2115–2118; f) T. D. Huber, J. A. Clinger, Y. Liu, W. Xu, M. D. Miller, G. N. Phillips Jr., J. S. Thorson, *ACS Chem. Biol.* **2020**, *15*, 695–705.

[19] R. Wang, K. Islam, Y. Liu, W. Zheng, H. Tang, N. Lailler, G. Blum, H. Deng, M. Luo, *J. Am. Chem. Soc.* **2013**, *135*, 1048–1056.

[20] F. Michailidou, N. Klöcker, N. V. Cornelissen, R. K. Singh, A. Peters, A. Ovcharenko, D. Kümmel, A. Rentmeister, *Angew. Chem. Int. Ed.* **2021**, *60*, 480–485; *Angew. Chem.* **2021**, *133*, 484–489.

[21] B. S. Chouhan, M. H. Gade, D. Martinez, S. Toledo-Patino, P. Laurino, *bioRxiv* **2020**, https://doi.org/10.1101/2020.08.17.254151.

[22] S. Hausmann, S. Zheng, C. Fabrega, S. W. Schneller, C. D. Lima, S. Shuman, *J. Biol. Chem.* **2005**, *280*, 20404–20412.

[23] G. Mayer, A. Heckel, *Angew. Chem. Int. Ed.* **2006**, *45*, 4900–4921; *Angew. Chem.* **2006**, *118*, 5020–5042.

[24] a) J. Schlesier, J. Siegrist, S. Gerhardt, A. Erb, S. Blaesi, M. Richter, O. Einsle, J. N. Andexer, *BMC Struct. Biol.* **2013**, *13*, 22; b) F. Wang, S. Singh, J. Zhang, T. D. Huber, K. E. Helmich, M. Sunkara, K. A. Hurley, R. D. Goff, C. A. Bingman, A. J. Morris, J. S. Thorson, G. N. Phillips, Jr., *FEBS J.* **2014**, *281*, 4224–4239; c) C. Minici, L. Mosca, C. P. Ilisso, G. Cacciapuoti, M. Porcelli, M. Degano, *J. Struct. Biol.* **2020**, *210*, 107462.

[25] M. Porcelli, C. P. Ilisso, E. De Leo, G. Cacciapuoti, *Appl. Biochem. Biotechnol.* **2015**, *175*, 2916–2933.

[26] X. Wang, Y. Jiang, M. Wu, L. Zhu, L. Yang, J. Lin, *Enzyme Microb. Technol.* **2019**, *129*, 109355.

[27] M. Porcelli, G. Cacciapuoti, M. Carteni-Farina, A. Gambacorta, *Eur. J. Biochem.* **1988**, *177*, 273–280.

[28] J. Deen, S. Wang, S. Van Snick, V. Leen, K. Janssen, J. Hofkens, R. K. Neely, *Nucleic Acids Res.* **2018**, *46*, e64-e64.